NASA TT F-8573

NASA TT F-8573

20p

~~X64 12474~~ refs

Code 5D

DESIGN PROBLEMS FOR A ONE-STAGE TRANSPORTER [*]

by

J. Lambrecht Nov. 1963 20p refs.

Transl. .. by Holman (John F.) and Co. " from

Double code
114 8482

Translation of "Probleme bei der Verwirklichung eines einstufigen Raumtransporters"
from Raketentechnik und Raumfahrtforschung, Vol. 7, No. 3, 107-114, 1963 p 107-114
(Stuttgart), v.7 no. 3

Presented at the 3d European ~~Congr.~~ Space Flight Congr., Stuttgart, May 1963

[redacted]

[redacted]

NATIONAL AERONAUTICS AND SPACE ADMINISTRATION

WASHINGTON, D. C. November 1963

DESIGN PROBLEMS FOR A ONE-STAGE SPACE TRANSPORTER[1] /107

J. Lambrecht

12474 author

It is expected that the present booster-rockets used for the launching of orbital payloads will be replaced by recoverable space-transporters, in order to keep the cost of the expanding spaceflight programs within economical limits.

In several countries, including Germany, a variety of different proposals has been made with the common aim of providing a method for launching payloads into orbit more economically than with booster rockets. These proposals include single and multistage systems. A solution of special technical elegance is a one-stage space-transporter capable of putting payloads into low earth-orbits and returning to its base similar to an airplane. Studies made in connection with the National Space Program, Research Project 623 (space-transporter), have indicated that, with proper selection of the climb path, winged space-transporters using launching aids may put a relatively high percentage of the starting weight into orbit. Requirements with respect to the mass ratio can be realized, if structural weights per unit area and wing sizes can be kept within certain limits.

Author

In the few years since the launching of the first satellite the tasks facing spaceflight programs and, therefore, the requirements on the carrying systems have grown in an extraordinary fashion. Both the United States and Russia have launched artificial satellites and space vehicles with rockets whose origin lies partly in the military arsenals of the respective countries and partly (particularly those to be used in future assignments) in special developments for space travel purposes. In cases when the payload is to be returned to earth, use is made of ballistic capsules resembling military warheads in their function. Thus, it can be seen that the technology employed for the carrying and reentry systems is closely related to the methods developed for military purposes. The reasons for this can be found in the resultant economy and in the time pressure originating from the competition between the United States and Russia.

[1] Translated from "Raketentechnik und Raumfahrtforschung," No. 3, pages ~~107-114, 1963.~~

The direction indicated by the two major powers is not suitable for Europe. To be sure, there is at the present time a European booster rocket under development, but this rocket, developed solely for the purpose of collecting data, must be launched in Australia. This emergency solution would be unacceptable if an intensive and concentrated European effort in this area of spaceflight were to be made, since the launchings would have to take place in Europe.

There are two major reasons - both closely related to the dense population in Europe - against the use of booster rockets. First, the return of the first stage back to earth and the very large area which must be reserved for the impact, and second, the lack of dependability. Both these problems can be solved simultaneously with a reusable carrier. In particular, the improvement of dependability to a degree corresponding to normal requirements in other areas of technology can be achieved only when reliance is not placed solely on simulated flight but when actual test flights can be performed.

There is still another factor, not necessarily limited to the European continent, which supports the use of reusable carriers; the /108
expenditures connected with spaceflight. The weight-per-year ratio of payloads placed into earth orbits (Figure 1) has reached substantial values in the last few years and should reach thousands of tons a year before the end of this decade. Even when it is considered that the cost per kilogram of payload decreases substantially (Ref. 3) with the use of larger rockets, as shown in Figure 2, the media employed for the booster rockets themselves (Figure 3) represent a considerable weight factor. The cost per kilogram of payload can, however, be substantially decreased through the use of recoverable carrier systems. The numerous proposals found in American trade publications show that this problem is of great importance in the United States. These proposals range from the winged Saturn stages (Figure 4), through the ASTRO Project (Figure 5), to the aerospace plane (Figure 6). The proposed projects vary between extremes which indicate that these projects are in the initial stages of study and development. It is assumed that serious work on the development of a reusable carrier system will begin in the United States at the earliest in 1965 (Ref. 1).

The importance of this problem is also recognized in Europe. In the Eurospace program (the association of European spaceflight industries), the project of developing a reusable carrier system (Project "Space-Transporter") has been given first priority among the various study projects (Ref. 2). The space-transporter is designed to place payloads into close-to-earth orbits and to return back to earth in reusable condition at a predetermined location. In addition, the space-transporter must be capable of recovering payloads from orbital paths (e.g., space-station crews). For reasons stated earlier, the space-transporter must be capable of rendezvous maneuvers for assembling large loads in space. Also, for the same reasons, it is desirable that the space-transporter be manned.

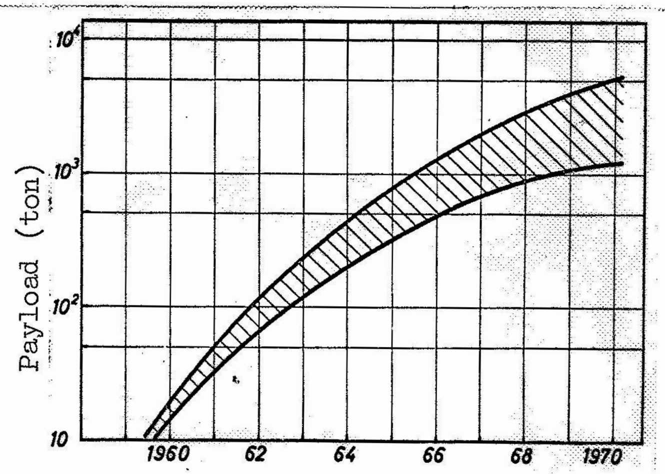

Figure 1. Total Annual Payload Weight Placed in Orbit.

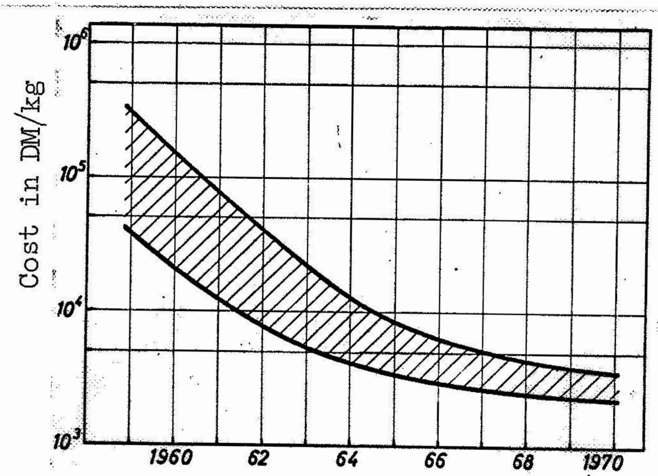

Figure 2. Evolution of Transport Cost per kg of Payload (Ref. 3).

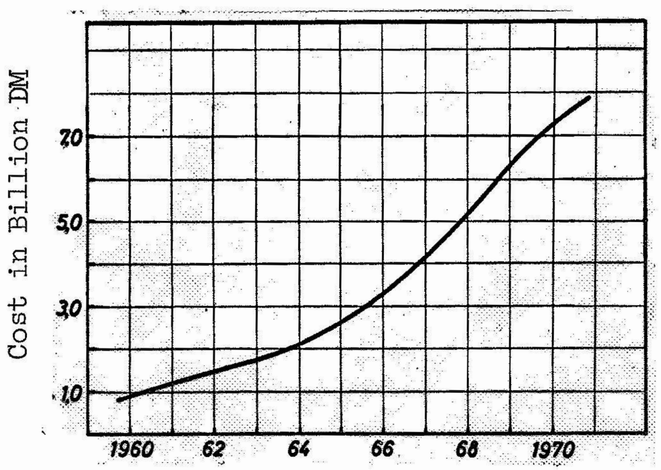

Figure 3. Probable Evolution of Annual Cost for Rocket Transported Payloads.

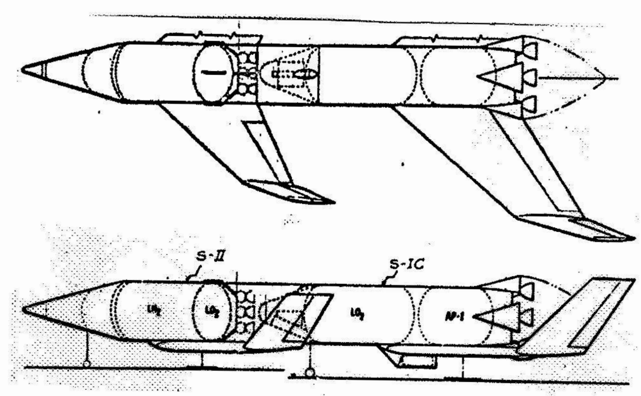

Figure 4. The Two-Stage Saturn C-5 Concept with both Stages Recoverable (Ref. 1).

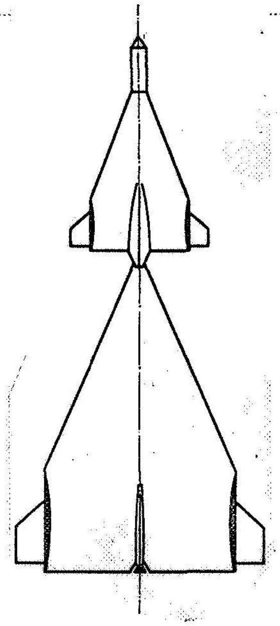

Figure 5. The Astro Concept of a Two-Stage Space Transporter Powered with O_2/H_2 (Ref. 6).

In Germany, a number of private firms are engaged in space-transporter projects. The versions under investigation include one- and two-stage systems which can be launched from vertical or horizontal positions. At the present time, the Junkers Company is considering a horizontally launched one-stage space-transporter which employs an auxiliary launching system (Figure 7). The auxiliary launcher could consist, for example, of a steam catapult.

In the following paragraphs some of the problems encountered in the development of a one-stage space-transporter are discussed. The craft is capable of delivering payloads into a 300-km circular orbit. /109

The characteristic climb velocity must be determined first. From that, the percentage of the launching weight is calculated by assuming a specific impulse. Then, conclusions regarding admissible specific structural weights and the size of the payload can be drawn. In particular, it will be possible to answer the important question of whether a horizontal or vertical launching is more favorable as regards the energy required.

Since computer programs for the analysis of climb paths, in which the air resistance and lift are taken into account, have not been available in the past, the escape velocities of the various climb paths had

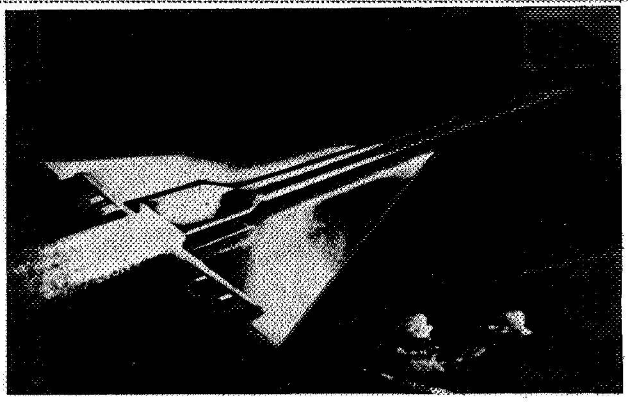

Figure 6. Typical Aerospace Plane Design.

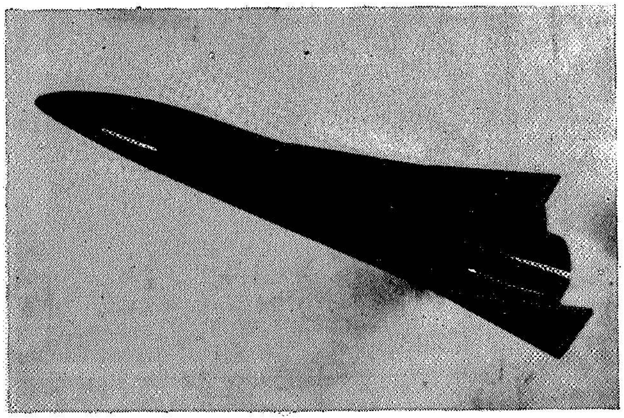

Figure 7. Single-Stage Rocket Propelled Space-Transporter.

to be computed manually with the application of certain simplifying assumptions. These assumptions were necessary to obtain integrable relations.

The forces acting on the space-transporter were separated into the accelerating force, mb; the part of the total load carried by the jet minus the centrifugal force, $m(g - V^2/R) \sin \alpha$; the part of the total weight carried by lift minus the centrifugal force $m(g - V^2/R) \cdot \epsilon^+ \cdot \cos \alpha$; the zero resistance W_o, and the thrust $w(dm/dt)$. The summation of the above results in:

$$-w\,(dm/dt) = mb + m\,(g - V^2/R) \sin \alpha + m\,(g - V^2/R)\, \varepsilon^+ \cdot \cos \alpha + W_o \tag{1}$$

Typed by AS
Proofread by
Corrections typed by
Corrections proofread by
Corrections put in by
Final check by

where $(90 - \alpha)$ is the angle between the velocity of flight and gravity vectors, ϵ^{+} is the ratio of the lift-dependent air resistance to lift, and w is the jet velocity. To carry out the integration over a time interval, it was assumed that the angle α is constant within the atmosphere up to an altitude of 50 km, and that the acceleration b is constant. The jet velocity vector coincides with the vehicle velocity vector. In addition, the ratio ϵ^{+} and the zero resistance coefficient C_{wo} had to be assumed constant. The variation in atmospheric density was assumed to be given by the approximation

$$\frac{\rho}{\rho_o} = \left(1 - \frac{H}{400000}\right)^{49}$$

where H is the altitude in meters.

It is obvious that these assumptions only very roughly correspond to the actual case. Consequently, the results obtained by means of these approximations should be viewed only as relative values while the absolute values are yet to be determined by exact methods. Nevertheless, as demonstrated in the following paragraphs, some of the results obtained by the approximate method show surprisingly good agreement with values which have appeared in American publications.

When the assumptions listed above are substituted into Equation (1), Equation (2), shown in Figure 8, results after some transformations. This equation is used for the flight in the atmosphere.

For altitudes beyond the atmosphere (i.e., for altitudes greater than 50 km), a bielliptical transition was employed (Figure 8). It was found that for the entire region of orbital paths under consideration, the apogee of the first ellipse is below 300 km. Thus, the propulsion was assumed shutoff at an altitude of 50 km and the flight was assumed to continue without propulsion to the apogee of the elliptical orbit. It was further assumed that upon reaching the apogee, an impulse is produced which accelerates the space-transporter into the final desired elliptical orbit with a 300-km apogee. There, a second orbital velocity-producing impulse was assumed to be given.

The method described above was used to perform calculations for various ratios ϵ^{+} with various accelerations over a range of climb angles. The result of these calculations is shown in Figure 9. When examining this diagram, it should be kept in mind that these results have been obtained by applying simplifying assumptions and, therefore, the significant result is the trend shown rather than the absolute values involved. The diagram contains three sets of curves denoted by different lines. Each set consists of three curves which are valid for the range of climb angles varying between 5^{o} and 60^{o}. The curves are discontinued

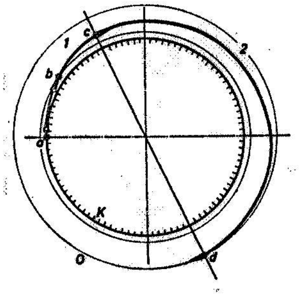

a-b: Climb path for a fixed angle (Equation 2, Impulse I)
b-c: Free-flight ballistic path
c: Impulse II given for transition from ellipse I to ellipse II
d: Impulse III given for transition from ellipse II to circular orbital path
k: Earth contour
o: Circular orbital path

Equation 2:

$$\ln\frac{m}{m_0} = \left[-\frac{1}{a}\cdot[b+g\cdot(\sin\alpha+\cos\varepsilon)]\cdot t\right] + \left[\frac{\sin\alpha\cdot\cos\alpha\cdot\varepsilon}{a}\cdot\frac{b^2 t^2}{R_0^2}\right]\cdot\left[\frac{F\,g_0\,c_w\,b^{\frac{1}{2}}}{2am}\left(\frac{800000}{\sin\alpha}\right)^{\frac{1}{2}}\cdot\int_0^v (1-v^2)^{4.2}\cdot v^2\,dv\right],$$

Figure 8. Intrinsic Bielliptical Flight Path Transition

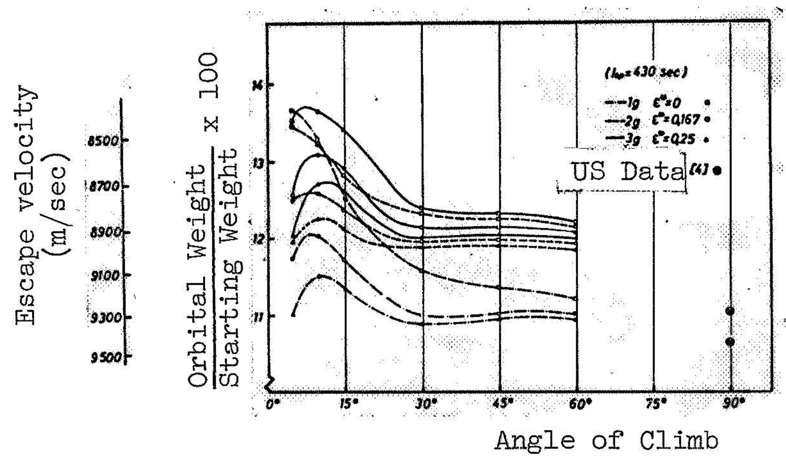

Figure 9. Escape Velocity vs. Percentage of the Starting Weight Placed in Orbit. (See text for assumptions made with reference to the climb path.)

at the 60° angle because, for steeper angles, the approximate methods furnish results which deviate greatly from the actual case. However, data taken from American sources (Ref. 4) are shown in the diagram and are seen to fit into the picture rather well. The constant angles of climb shown in Figure 9 should be regarded as the average values of the variable angles of climb which occur in the actual case.

Each set of curves is valid for constant accelerations of 1, 2, and 3 g respectively, as shown by the legend; the curves are valid up to a 50-km altitude. In each case, the lowest curve is valid for the case $\epsilon^+ = 0.25$, the middle curve for $\epsilon^+ = 0.167$, and the uppermost curve for

$\epsilon^+ = 0$. The uppermost curve corresponds to the impossible-to-attain upper boundary, and the values of ϵ^+ between 0.25 and 0.167 can, in all probability, be realized in the super and hypersonic regions. Thus, in each case, the region of particular interest is between the two latter curves. As was mentioned earlier, the acceleration will hardly be constant during an actual flight. However, the constant acceleration used in the calculations for reasons of simplicity can be viewed as the average value of accelerations produced by constant thrust. For example, a constant acceleration of 1 g can be regarded as the average value for a constant thrust which produces an initial acceleration of around 0.3 g and a final acceleration of 2 to 3 g. Correspondingly, one could regard a constant acceleration of 3 g as roughly equivalent to a constant thrust producing an initial acceleration of around 1 g and a final acceleration of 8 to 10 g. The above figures should be viewed as being indicative of the possible range rather than as rigidly fixed correlations.

In examining Figure 9, it should be recognized that for climb angles /110 greater than 10° to 15°, higher accelerations will lead to a percentage of higher orbital masses and are therefore favorable. This follows from the fact that higher accelerations will cause a decrease in the climb duration time with a corresponding decrease in the gravitational effects. The effect of the increased air resistance resulting from an increase in acceleration is smaller than the effect of gravitational forces in the region under consideration. On the other hand, it can be seen that the gain in orbital mass resulting from raising the average acceleration from 2 to 3 g is rather small in this region. Therefore, it should be anticipated that for still higher accelerations the effect of the increased air resistance will cause a further decrease in the orbital mass.

This effect can be recognized in the case of small climb angles. The curves for 2- and 3-g accelerations intersect in the neighborhood of the 5° angle, which indicates that the effect of air resistance begins to predominate. It is also interesting to note that for $\epsilon^+ = 0$ (i.e., for the zero resistance case) the curves corresponding to 1 g and 2 g accelerations already intersect in the vicinity of a 10° angle. Perhaps it may be added here that the curves obtained by the Junkers Company appear to be in good agreement with the American data (Ref. 4) given for vertically-launched spacecraft. If one supposes that the American devices were launched at an initial acceleration of about 3 g which, as mentioned earlier, corresponds to our curves for 1-g constant acceleration, then the American data would fall on the extension of the 1-g constant acceleration curves. As a result, it is hoped that the curves shown in Figure 9 are representative not only with regard to their general shape, but also with regard to their values. This supposition is presently being investigated.

Having considered the relative positions of the curves with respect to one another, we shall turn our attention to their general form. It is seen that all of the curves are relatively flat in the interval from 30° to 60°. At the angle of 30°, a larger part of the weight is carried by lift than at the angle of 60°; on the other hand, the duration of climb and the air resistance are greater at the shallower angle of climb. These effects are of about the same order of magnitude in the region between 30° and 60° and tend to balance each other. The weight begins to be carried predominantly by lift rather than by thrust only at angles smaller than 30°, in spite of the increased air resistance and duration time, with the net effect of a considerable gain in percentage orbital mass. However, at very small angles this advantage is again lost because of the increased duration time and air resistance effects, and the percentage orbital weight becomes smaller. The maxima (i.e., the points of maximum percentage orbital weight) are seen to shift with increasing ϵ^+ in the direction of the increasing angle of climb for each group of constant acceleration curves. This effect can be explained simply by noting that the air resistance significantly increases with increasing ϵ^+. On the other hand, the effects of air resistance increase with the angle of climb, thus shifting the optimum to the right. The control calculations for $\epsilon^+ = 1.0$, which have not been shown in the diagram for reasons of clarity, indicate that the optimum point for higher values of ϵ^+ moves rapidly toward the steep climb angles so that for $\epsilon^+ = 1.0$ the optimum is in the area of the 60° angle.

The characteristic escape velocity for each angle of climb can be obtained from Figure 9 for each fuel combination. The fraction of the starting weight brought into orbit can be calculated for any specific impulse with the fundamental rocket equation.

The ordinate scale used in Figure 9 corresponds to a specific impulse of 430 sec; an attainable value with an O_2/H_2 fuel combination, if a high-pressure power plant is used. However, an investigation of the effect of fuel mixture ratios on the size of the space-transporter and on the cost per kilogram of payload has indicated that the most favorable fuel mixture ratio for the O_2/H_2 combination is about 7:1. This is also confirmed by other sources (Ref. 4). For this particular mixture ratio, the value selected as the specific mean impulse appears to be somewhat high. Reducing the specific mean impulse to 410 sec (this value should be attained by the end of this decade) would make the percentage orbital weight smaller by about 1 percent. However, this loss can be compensated for by employing a catapult launching aid, in which case the values given by Figure 9 can be taken as representative for a space-transporter which is launched with the aid of a catapult and is powered by the O_2/H_2 fuel combination in a 7:1 mixture ratio. It should be further mentioned that the beneficial effect of the earth's rotation on the escape velocity had not been taken into consideration in constructing the curves. Thus, the data shown represent a polar orbital path.

The results of the investigation of the effects of acceleration and of the angle of climb on the percentage orbital weight show that the start from a horizontal position accompanied by a relatively shallow angle of ascent is more favorable than a vertical start for a vehicle whose configuration is such that the aerodynamic lift produced is greater than the air resistance. The data, taken from American sources, which demonstrate that the percentage orbital mass increases from about 11 percent for a vertical start to over 12 percent for a horizontal one are of great significance if one considers that the payload constitutes a maximum of 1 percent of the starting weight.

If it is postulated that the air frame constitutes the same fraction of the total weight for both possible launching positions and that the required proportions can be attained at all, then, in selecting the climb path, it is no longer a question of the size of the payload, but a question of whether the payload can be carried at all. It is known that percentage orbital masses in excess of 13 percent are attainable with a constant acceleration of 3 g (involving an escape velocity smaller than 8600 m/sec). These figures are still to be confirmed by exact calculations and it is still to be found whether the demands on orbital paths corresponding to this average acceleration can be met.

The following discussion is concerned with the specific case of an escape velocity of 8860 m/sec and a percentage orbital mass of 12.2 percent (a fuel percentage of 87.8 percent) which, according to Figure 9, is a fully attainable value. One can compare these with the fuel percentages of 88 percent for the first stage and 86 percent for the second stage cited in reference 4, in connection with the Douglas project ASTRO. /111
For a second considered fuel combination, we take F_2/N_2H_4 in a mixture ratio 2.2:1, a calculated velocity of jet of 3950 m/sec corresponding to a specific impulse of 403 sec from which the percentage orbital mass is calculated at 10.6 percent for the escape velocity of 8860 m/sec. The fuel percentage for this case is seen to be higher and this fact makes the fuel combination F_2/N_2H_4 appear, at first glance, unfavorable. However, in the following discussion it will be shown that this disadvantage is more than offset by the higher density of F_2/N_2H_4.

Figures 10 and 11 have been selected from among a number of similar diagrams. They represent a survey of admissible structural weights for the two fuel combinations O_2/H_2 and F_2/N_2H_4 and, therefore, the percentage orbital masses of 12.2 percent and 10.6 percent respectively. The problem is reduced to the interpretation of geometrical relationships. The structure of the diagrams is explained in Figure 10 (the O_2/H_2 case). The diagram relates the starting weight G_o to the load per surface area,

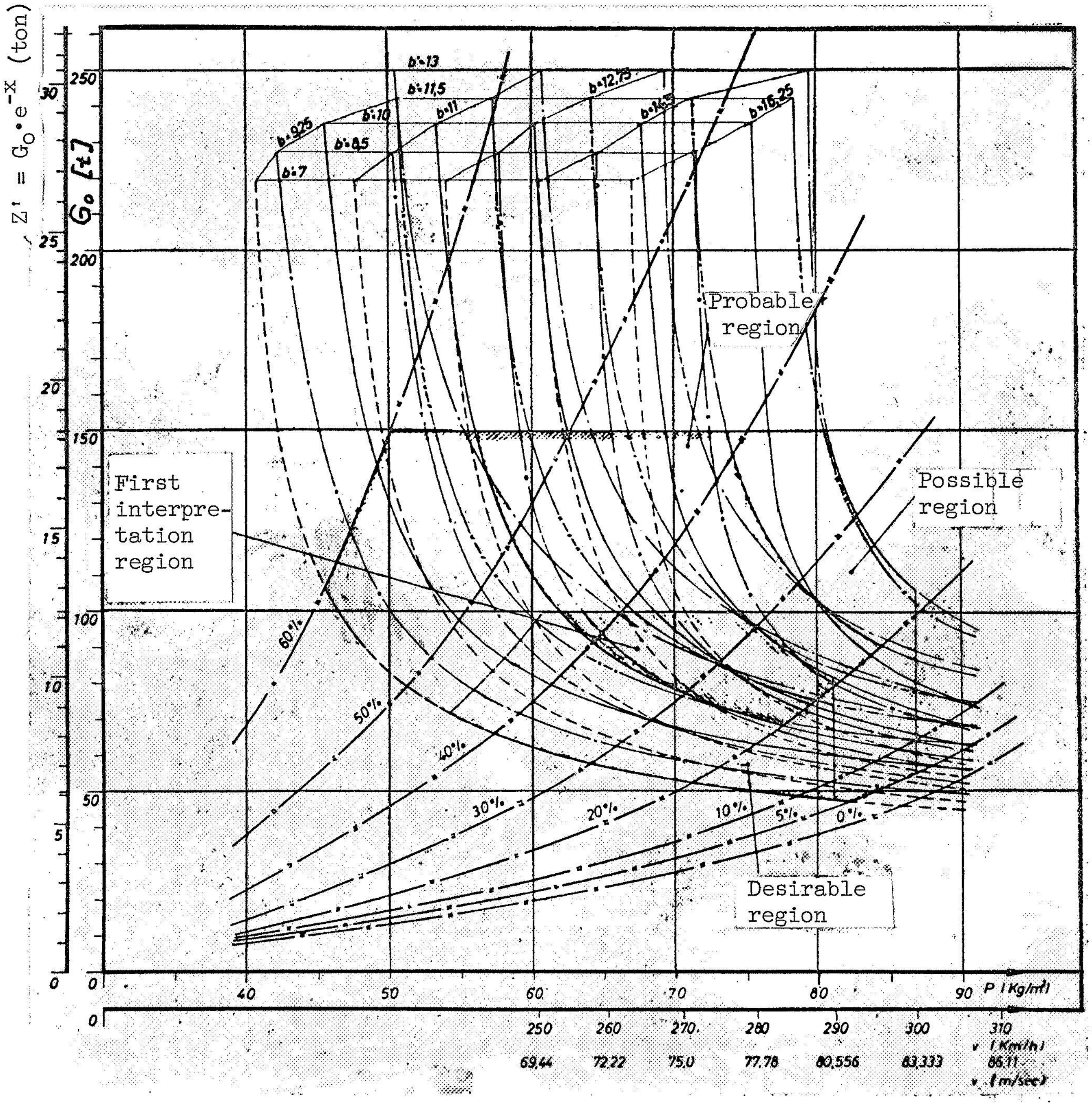

Figure 10. Space-Transporter (O_2/H_2) Starting Weight as a Function of Surface Loading p for Various Specific Structural Weights of the Fuselage (b') and Lifting Surfaces (b). Drag Length of Fuel Tank L_r = 14.3 km

Typed by ____________
Proofread by ____________
Corrections typed by ____________
Corrections proofread by ____________
Corrections cut in by ____________
Final check by ____________

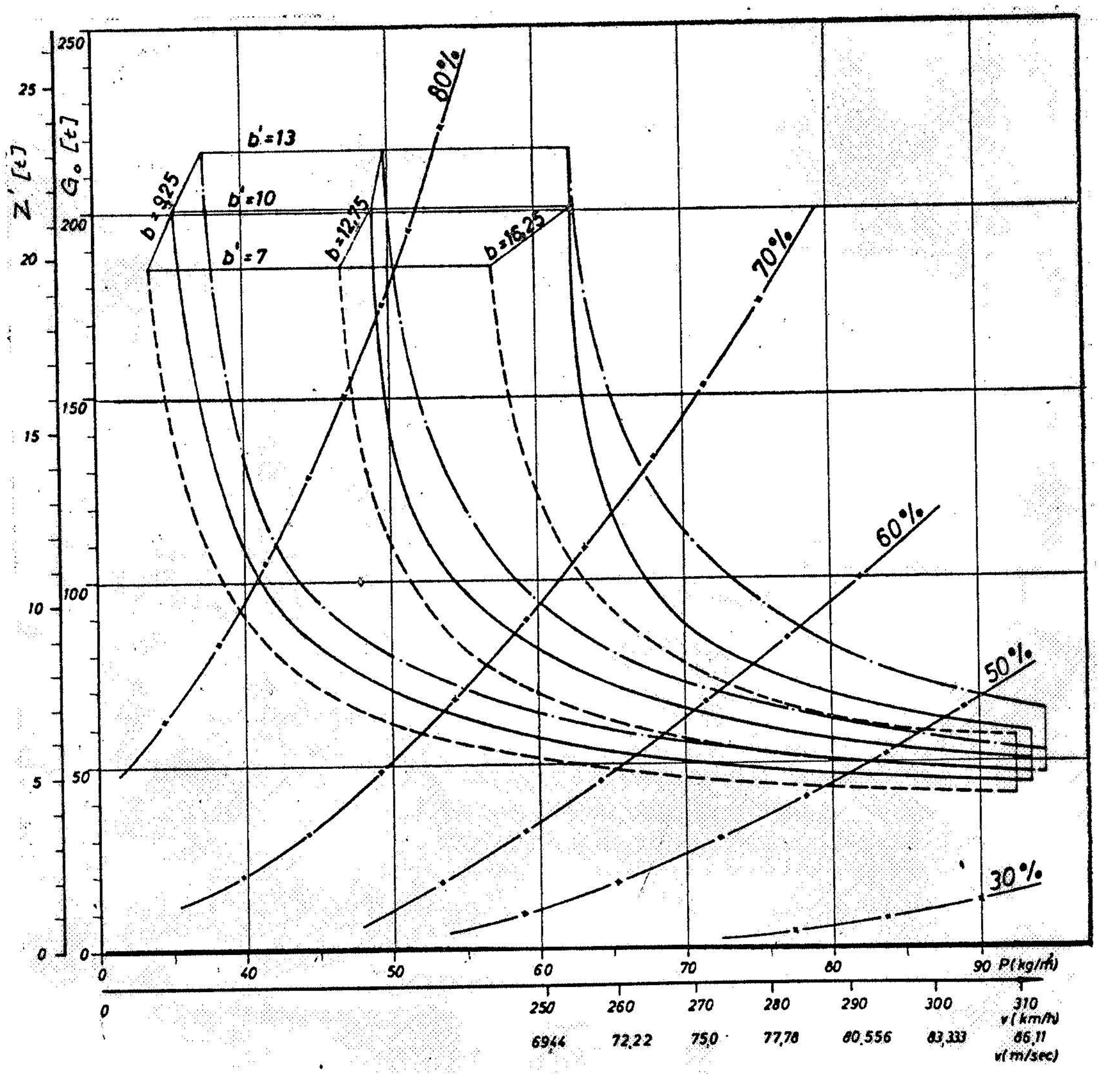

Figure 11. Space-Transporter (F_2/N_2H_4) Starting Weight as a Function of Surface Loading p for Various Specific Structural Weights of the Fuselage (b') and Lifting Surfaces (b). Drag Length of Fuel Tank L_r = 14.3 km

P, at landing. The values of G_o, given by the inner scale, are plotted as ordinates with the values of P given by abscissas. The outer scales are the equivalent scales correlating the orbital weight with the landing speed. The curves drawn with various dashed lines represent fixed combinations of structural weights used for the fuselage b' and the wetted surface of the weight carrying surfaces including the surface b of the underside of fuselage. The drag length of the fuel container is assumed to be 14.3 km, and the fuel tank is assumed to be in the shape of a circular cylinder with a length/diameter ratio of 8.5. Furthermore, the diagrams contain curves of the so-called constant supplementary areas; i.e., the percentage contribution of the sweptback wings in comparison with the total area of the carrying surface. The remainder of the carrying surface is provided by the fuselage underside.

In calculating the starting weight G_O, the following fixed weights (in metric tons) were assumed:

Rocket engines	$G_R = 0.051\ G_O^{2/3}$,
Landing gear	$G_F = 0.017\ G_L$,
Electric and hydraulic plants	$G_A = 0.015\ G_L$,

where G_O is the starting weight and G_L is the weight placed into orbit, and:

Cabin	$G_K = 0.9$,
Crew	$G_B = 0.3$,
Electronic equipment	$G_E = 0.3$,
Payload	$G_N = 0.5$.

/112

The pure payload (i.e., the weight which is either placed into orbit or brought back to earth) was assumed as 500 kg in the calculations. The relatively low payload can be explained by the fact that the desired maximum starting weight was, at first, determined to be 100 tons. Investigations involving larger payloads have indicated that the starting load does not increase in proportion with the payload. This point will be considered in detail later on.

To begin with, Figure 10 shows that the shape of all curves representing fixed combinations of specific structural weights has a hyperbolic character; i.e., there are regions in which the curves are relatively flat and regions in which the curves rise steeply. In cases where the contribution of the supplementary lifting surfaces is large (see the 60 percent curve), the starting weight increases rapidly. This is because of the increase in the required flexural rigidity of the tank as the tank increases in size. These stiffness requirements are obviously related to the length/diameter ratio of the tank. For more compact tank forms, this rapid rise takes place at greater values of the starting weight. A similar rapidly rising curve will, incidentally, be obtained when a certain definite payload weight is exceeded, as will be shown later.

It is of particular importance to limit the size of the supplementary lifting surfaces to the absolute minimum necessary to ensure stability and steerability. A small size of the supplementary surfaces causes no problems during launching and landing operations. The admissible specific structural weights should, quite naturally, be kept low; however, it should be noted that the specific structural weights for the supplementary lifting areas are given in terms of weight (kg/m^2) per wetted surface, which means that these values will double when projected areas are considered. When it is considered that the space-transporter is not required to perform maneuvers producing multiple loadings of high intensity, there is hope that the requirements with respect to the specific structural weights can be met. Structural analysis of the tanks has produced weights which are compatible with the previous remarks. Structural analysis and weight estimates are presently being prepared. For the fuselage, the situation is quite similar. In this case, however, it is assumed that the body is self-supporting so that the skin of the fuselage serves principally as a protective coating against the aerodynamically generated high temperatures.

The several regions shown in Figure 10 are: the possible region which covers practically the entire range of parameters used in this analysis, but which is bounded on the top by the starting weight of 150 tons; the probable region in which the estimates cancel each other; the desirable region (i.e., the region to be strived for, which is bounded on the top by what appears to be the desirable starting weight of 100 tons; and finally, the region in which the results can be viewed as a superposition of all the other regions and in which the first interpretation should be made. The middle point of the region of first interpretation corresponds to the following:

Starting weight	85 tons
Percentage contribution of the supplementary lifting surfaces	30 percent
Specific structural weight of the fuselage, b'	10 kg/m^2
Specific structural weight of the lifting surface, b	12.75 kg/m^2
Landing speed	275 km/hr

/113

Figure 11 shows similar results for the same range of specific weights, but for the fuel combination F_2/N_2H_4 with a 2.2:1 mixture ratio. Again the resulting curves are seen to resemble hyperbolas. It is noteworthy that, in this case, the curves have moved closer together (signifying that the effect of the specific structural weights is of somewhat lesser importance), and that the curves have also shifted in the direction of the lower surface loadings. Both of these phenomena are the consequence of the higher density of fuel and the resulting smaller dimensions of the craft (see also Figure 12). Since the dimensions of all surfaces are relatively small in this case, the effect of structural weights must also be small.

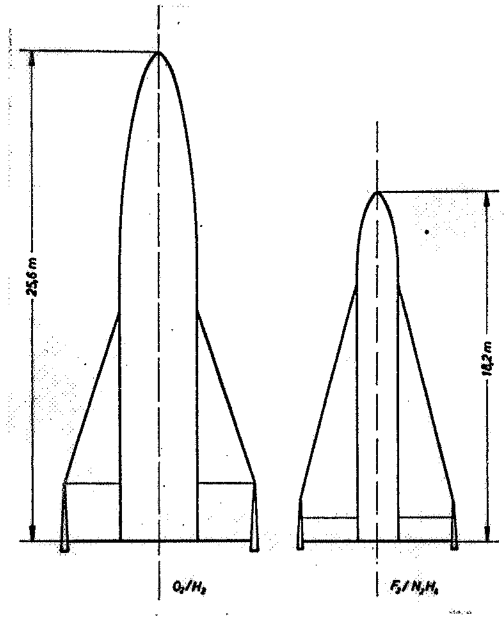

Figure 12. Space-Transporter Size Comparison for Two Fuel Combinations

In addition, it is gratifying to note that the region in which the curves rise steeply can, in all probability, be neglected. It can be seen that the percentage load carrying capability of the supplementary surfaces is quite large in the entire region; it generally exceeds 50 percent. This demonstrates the beneficial effect of the high density of the F_2/N_2H_4 fuel combination on the tank size and, therefore, on the entire concept of the space-transporter. Also, no particular difficulties can be anticipated with regard to stability and steerability of the transporter because of the large size of the supplementary lifting surfaces. Consequently, the parameter determining the size of the supplementary surfaces could very well be the landing speed in this case.

For comparison purposes, Figure 12 shows two space-transporters designed to carry a 500-kg payload, with one transporter using the O_2/H_2 fuel combination mixed in a 7:1 ratio, and the other using the F_2/N_2H_4

fuel combination mixed in a 2.2:1 ratio. In both versions, the specific structural weight of the fuselage is 10 kg/m^2 and that of the supplementary lifting surfaces is 12.75 kg/m^2 of the wetted surface. A supplementary lifting surface of 30 percent was assumed for the O_2/H_2 version and a landing speed of 290 km/hr for the F_2/N_2H_4 powered version. The starting weights for the two craft are 85 tons and 50 tons respectively. It is clear that the space-transporter powered by F_2/N_2H_4 is, as should have been expected, not only smaller in size than its O_2/H_2 counterpart, but, in spite of the smaller specific impulse which it can produce, still has a lower starting weight. It is obvious that despite the 7:1 mixture ratio, the low specific weight of the O_2/H_2 combination is a substantial disadvantage in this case.

Although the F_2/N_2H_4 fuel combination is superior to the O_2/H_2 combination as far as the weight, size, and, probably, constructional difficulties are concerned, there is one factor that speaks strongly in favor of the latter fuel combination--the comparative costs of fuel elements. If one takes the previously listed starting weights, fuel combinations, and mixture ratios and assumes the following costs of fuel elements, the resulting fuel cost per launching for the O_2/H_2 version is DM 4,800, while the cost for the F_2/N_2H_4 version is DM 304,000:

O_2	0.16 DM/kg
H_2	4 DM/kg
F_2	8 DM/kg
N_2H_4	2 DM/kg.

Thus, the advantage of the O_2/H_2 combination is an economic one. However, it must be kept in mind that the air frame cost, the development costs, and the launching costs play an important role in the total cost of the device and should be lower for the smaller craft. It is not presently known how the total costs per launching of the two versions compare. This problem is presently under scrutiny.

It was previously emphasized that the starting weight increases with an increase of the payload weight. Our investigations show that, initially, an increase in the payload weight beyond the selected value of 500 kg produces an increase of the payload/starting weight ratio. This is easily explained by the fact that the payload comprises only a small part of the total weight carried by the space-transporter. Above a certain payload weight which, depending on the selected configuration for the craft, does not necessarily have to be very large, the starting weight grows more rapidly than the payload weight. This rapid growth of of the starting weight is caused by the rapidly growing strength requirements dictated, in turn, by the increase in size of the craft. As a result of this, the payload/starting weight ratio tends to decrease again.

Results of similar nature can be found in American sources. Particular attention is called to the diagram in Figure 13. This diagram shows the qualitative relationship between the payload and starting weight for vertically and horizontally launched vehicles without giving any quantitative data (Ref. 1). Both versions represented in Figure 13 land in a horizontal position. The two curves show that a rise in the payload/starting weight ratio is to be expected initially and that, afterwards, the starting weight begins to strongly increase until a maximum payload is reached. Furthermore, it is very interesting to note that, according to this source, a horizontally launched space-transporter carrying a small payload and aided by aerodynamic lift requires smaller starting /114
weights than the vertically launched craft. In other words, the escape velocity of a horizontally launched space-transporter is smaller than that of the vertically launched one--a result which already had been demonstrated by Figure 9. Unfortunately, Figure 13 gives only a qualitative relationship. The only clue of a quantitative nature furnished by the source is the mention of the range of payload weights in which the two curves of Figure 13 intersect; namely, 13.5 to 18 tons for two-stage rockets with both stages driven by liquid propellants. If one assumes that the payload percentage of a two-stage rocket is in the order of 3 to 4 times that for a one-stage rocket, the maximum payload obtained from this diagram coincides with the values we calculated throughout the entire range.

An attempt had been made to list the reasons supporting the development of a reusable European space-transporter. Even though no final conclusions with regard to the system to be selected can be made now, some very interesting results have been obtained. Of particular interest are the results obtained from investigations carried out within the framework of the National Spaceflight Program, which show that the orbital mass can be made larger by employing a horizontally launched vehicle which is aided by aerodynamic life. Diagrams, from which the starting weight and surface loading can be read for various specific structural weights, have been constructed for a one-stage space-transporter with a launching aid and powered by O_2/H_2 or F_2/N_2H_4 fuel combinations. In this connection,

it was found that the size of the lifting surface is determined by

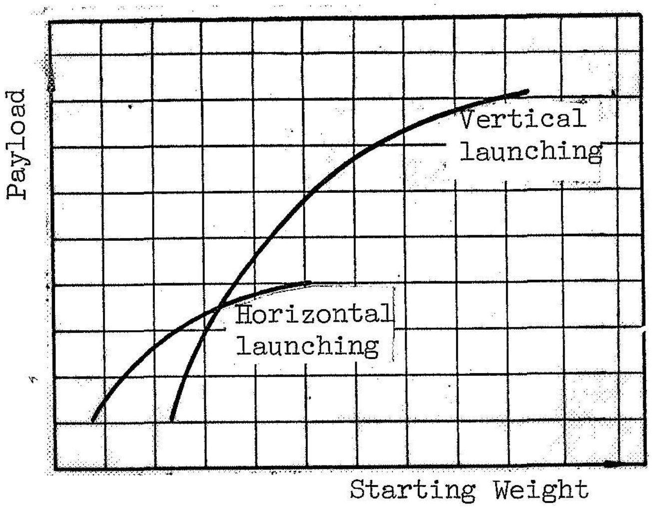

Figure 13. Payload as a Function of Starting Weight for Vertical and Horizontal Launching

stability considerations for the O_2/H_2 version and by landing speed considerations for the F_2/N_2H_4 version. Additional intensive research is necessary before one of the two versions can be selected. The various fuel combinations have been considered at length in this report. Calculations with regard to the admissible flight path must be performed, and stress requirements for the various phases of flight, particularly those occurring during reentry, must be considered in detail so that dependable data for research, testing and construction will be available. The far reaching consequences of making a single selection make it imperative to continue with research in all related areas before the most favorable concept can be found. For example, the experimental laboratories and design offices are presently attempting to determine whether the required specific structural weights can be realized, whether the proposed self-supporting tank with temperature protection constitutes a truly advantageous solution, and which configuration of the system is the best.

It has been attempted here to describe only those few isolated problems of the system analysis which appear to be of particular importance. To realize a project of such magnitude, many more problems, such as guidance, telemetry, navigation, equipment, etc., must be solved. A discussion of any of these special problems would be beyond the scope of this report.

Typed by ________ Corrections proofread by ________
Proofread by ________ Corrections cut in by ________
Corrections typed by ________ Final check by ________

BIBLIOGRAPHY

1. Tinnans, M. Reusable Launch Systems. Astronautics, January 1963.
2. EUROSPACE-Bericht, 1963.
3. Koelle, H. H. Raketentechnik und Raumfahrtforschung, Vol. III, No. 4, 1959.
4. Plattner, C. M. Large Reusable Booster Designs Studied. Aviation Week, 4, February 1963.
5. Aviation Week, June 19, 1961.
6. ORDWAY Advances in Space Science and Technology, Vol. 3.

(Manuscript submitted on May 17, 1963--presented at the 3rd European Spaceflight Congress, Stuttgart, May 1963--DGRR-Preprint No. 1502(63)--Author's address: Dipl.-lng Jürgen Lambrecht, Junkers Aircraft and Motor Works AG, Munich, Franz-Joseph Str. 1.)

Translated for the National Aeronautics and Space Administration by John F. Holman and Co. Inc.